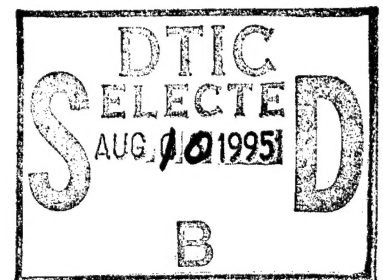AD

FRACTURE TESTING OF METALS AND COMPOSITES: TESTS AND ANALYSES FOR FAILURE PROBLEMS WITH ARMAMENT COMPONENTS

J.H. UNDERWOOD

DTIC
SELECTED
AUG. 10 1995
B

MARCH 1995

US ARMY ARMAMENT RESEARCH,
DEVELOPMENT AND ENGINEERING CENTER
CLOSE COMBAT ARMAMENTS CENTER
BENÉT LABORATORIES
WATERVLIET, N.Y. 12189-4050

BENÉT LABS

19950807 016

DTIC QUALITY INSPECTED 5

DISCLAIMER

The findings in this report are not to be construed as an official Department of the Army position unless so designated by other authorized documents.

The use of trade name(s) and/or manufacturer(s) does not constitute an official indorsement or approval.

DESTRUCTION NOTICE

For classified documents, follow the procedures in DoD 5200.22-M, Industrial Security Manual, Section II-19 or DoD 5200.1-R, Information Security Program Regulation, Chapter IX.

For unclassified, limited documents, destroy by any method that will prevent disclosure of contents or reconstruction of the document.

For unclassified, unlimited documents, destroy when the report is no longer needed. Do not return it to the originator.

REPORT DOCUMENTATION PAGE

Form Approved
OMB No. 0704-0188

1. AGENCY USE ONLY (Leave blank)	2. REPORT DATE March 1995	3. REPORT TYPE AND DATES COVERED Final

4. TITLE AND SUBTITLE
FRACTURE TESTING OF METALS AND COMPOSITES:
TESTS AND ANALYSES FOR FAILURE PROBLEMS
WITH ARMAMENT COMPONENTS

5. FUNDING NUMBERS
AMCMS: 6111.02.H611.1

6. AUTHOR(S)
J.H. Underwood

7. PERFORMING ORGANIZATION NAME(S) AND ADDRESS(ES)
U.S. Army ARDEC
Benét Laboratories, AMSTA-AR-CCB-O
Watervliet, NY 12189-4050

8. PERFORMING ORGANIZATION REPORT NUMBER
ARCCB-TR-95022

9. SPONSORING / MONITORING AGENCY NAME(S) AND ADDRESS(ES)
U.S. Army ARDEC
Close Combat Armaments Center
Picatinny Arsenal, NJ 07806-5000

10. SPONSORING / MONITORING AGENCY REPORT NUMBER

12a. DISTRIBUTION / AVAILABILITY STATEMENT

Approved for public release; distribution unlimited

12b. DISTRIBUTION CODE

13. ABSTRACT (Maximum 200 words)
Fracture tests have been broadly applied to failure of armament, including failures caused by each of the three general types of fracture--fast fracture, fatigue cracking, and environmentally-assisted cracking. This report describes some fracture mechanics tests and related analyses that have been useful to characterize fracture in armament components made from high strength steels and carbon/epoxy laminates. These include J-integral fracture toughness, notch fatigue life, and environmentally-assisted cracking tests and analyses for steels and linear elastic fracture toughness tests for laminates.

14. SUBJECT TERMS
Fracture Mechanics, Fracture Tests, Structural Metals, Composite Materials,
J-Integral Fracture Toughness, Fatigue Cracking, Environmental Cracking

15. NUMBER OF PAGES
23

16. PRICE CODE

17. SECURITY CLASSIFICATION OF REPORT	18. SECURITY CLASSIFICATION OF THIS PAGE	19. SECURITY CLASSIFICATION OF ABSTRACT	20. LIMITATION OF ABSTRACT
UNCLASSIFIED	UNCLASSIFIED	UNCLASSIFIED	UL

TABLE OF CONTENTS

Tables

List of Illustrations

i

INTRODUCTION

A variety of fracture mechanics-based tests and associated analyses has been used to address fracture problems with armament components. Fracture is often encountered with the guns and gun support structures in armament because service loads can approach the ultimate load of the component, and cyclic loads and sustained loads are often applied. Thus, each of the three general types of fracture--fast fracture in response to high load, fatigue cracking in response to cyclic load, and environmentally-assisted fracture in response to sustained tensile load in an aggressive environment--has been observed. The materials traditionally used in armament are high strength metal alloys. These are gradually being supplemented by composite and ceramic materials since lighter weight and higher performance armament components are required.

The variety and severity of loading and service environment and the different materials used with armament components have resulted in frequent use of fracture mechanics test and analysis methods to describe failures. The objective of this report is to describe some methods found to be particularly useful for describing failure in armament. Each of the three types of failure and two classes of materials already mentioned is included by briefly describing fracture case studies and research results from recent work. Fast fracture, fatigue cracking, and environmental fracture of alloy and stainless steel components are described first, followed by results from recent interlaboratory tests of the translaminar fast fracture behavior of carbon/epoxy composite laminates.

FRACTURE METHODS FOR STEELS

Three Useful Methods

Three generic types of fracture tests have been extensively used and reported in the technical literature. Fast fracture tests and analysis using J-integral methods are widely used (ref 1); fatigue crack initiation and growth methods have been applied to many types of materials and structures (ref 2); and environmental crack growth tests have been described (ref 3). With risk of over-simplification, three specific test and analysis methods are described that have provided simple yet definitive descriptions of fracture in armament components. Of course these methods are not ideal for all situations, but they can be used for most with a minimum of specialized test equipment and procedures.

Figure 1 shows the key elements of a compliance unloading J_{Ic} test used in failure analysis of a stainless steel welded structure (ref 4). Some details are given later. Two important points for the topic here, summarized in Figure 1, are as follows. First, the three-point bend configuration, generally regarded as quite simple to test, can now be used with a single, direct displacement measurement, V, at the crack mouth. Recent work (refs 5,6) has shown that V can be used for J calculation as well as its accepted use in compliance unloading. This avoids the difficulties with measuring load-line displacement. Second, the compliance-unloading method allows crack growth measurement throughout the test. The test in Figure 1 used a relatively small specimen, with $W = 10$ mm, so that the crack growth caused large increases in crack length, a, relative to W, and the decrease in slope of the unloads related to the increase in a/W

1

can be clearly seen. Note that even the occurrence of unstable cleavage fracture during the test can be described by the unloading compliance method.

A summary of fatigue initiation results for the same welded structure mentioned previously (ref 4) is shown in Figure 2. The $K/\sqrt{r}$ analysis used by Barsom and Rolfe (ref 2) for low and medium strength steel structures gives a good description of the measured fatigue initiation lives for bend specimens of four different weld and plate samples of high strength stainless steel. The quantity ($1.12\ K/\sqrt{r}$) is a good estimate of the maximum stress at the notch root, based on the stress intensity factor, K, and the notch root radius, r. By using the ratio of the maximum notch root stress to material yield strength, an S-N plot of results from four different materials gives a single trend line that can be used for descriptions of fatigue initiation life and for life predictions for the courageous.

Test and analysis methods for describing environmentally-assisted cracking are addressed in Figure 3. Shown are the bolt-loaded compact test configuration and applied K versus exposure time results for environmental cracking in a nickel-chromium-molybdenum high strength steel (ref 7). The bolt-loaded test is both simple and portable, which are considerable advantages when dealing with aggressive environments such as the warm acids in this example. An accurate K expression is available in terms of crack mouth displacement, V, rather than in terms of load, P, as is typical. As the crack grows with increasing exposure time, the applied K value decreases until a constant value is obtained, and this gives the value of K_{Ieac}, the threshold K for environmentally-assisted cracking for this material and environment. Note in the results here the starting value of applied stress intensity factor, K_o, has no effect on K_{Ieac}, because considerable crack growth has occurred at low K and the crack has grown beyond any effect of the prior higher K_o value.

This brief summary of J_{Ic}, notch fatigue, and environmental cracking test and analysis methods was intended to highlight three specific fracture analysis methods that have proved useful in prior work and have general, but not universal, utility. Additional information on the related fracture case studies is given in upcoming sections.

Fatigue and Fracture of Stainless Steel Welds

A failure of the main welded box beam of a gun carriage occurred by fatigue crack initiation and growth and subsequent fast fracture of the welds over a significant portion of the beam cross section (ref 4). A key part of the tests and analyses conducted in response to the failure was a series of fatigue initiation life and J_{Ic} tests, summarized in Table 1. Partial penetration welds in the box beam produced notches that became the initiation points for fatigue cracks, so notched bend specimens of the type sketched in Figure 2 were used for fatigue initiation tests. Initiation was defined as the number of cycles required for a crack to form at the notch root and grow across the 3-mm thickness of the weld. Later, the crack was grown further and the same samples were then used for J_{Ic} tests, as indicated in Figure 1.

Results are shown in Table 1 for three heat treat conditions of 17-400 precipitation hardening stainless steel weld metal (AMS 5825 specification). As anticipated, the lowest initiation lives were obtained for the welds where the solution heat treatment was omitted, as sometimes happens in the case of a weld repair. The subsequent J_{Ic} tests also showed this

omission of the solution heat treatment to give the worst results. The applied J versus Δa plots from which the J_{Ic} values were obtained are shown in Figure 4. Note that, as in the similar case discussed in relation to Figure 1, unstable cleavage fracture occurred for the weld-age heat treatment, leading to the lowest J_{Ic} value. In addition, the J values beyond the J_{Ic} point, such as at $\Delta a = 1$ mm (in Table 1), are significantly lower for the weld-age treatment.

Table 1 - Summary of Initiation Fatigue Life and J_{Ic} Fracture Toughness For Precipitation Hardening Stainless Steel Welds

Material	Condition	Initiation Life Cycles	J_{Ic} KN/m	J at $\Delta a = 1$mm KN/m
17-400	weld, treat, age	22,000	140	210
17-400	as welded	20,000	100	180
17-400	weld, age	14,000	75	75

As a result of the failure investigation of the welded cannon carriage, it was recommended to use deeper penetration welds, to perform the complete solution treat and ageing procedure whenever possible, or if not possible, then to apply much stricter inspection criteria to the carriage.

Environmental Fracture of a Cannon Tube

A quite unanticipated failure of a cannon tube occurred during a chromium plating process (ref 7). The tube was under no externally applied load whatsoever, and still a 1.7-m long crack grew entirely through the 48-mm thick wall of the tube. The test conditions eventually found to be crucial are shown in Figure 5 and listed in Table 2. The tube had a notch on the outer surface whose severity is only a little exaggerated (for clarity of presentation) in Figure 5. The tube also had circumferential direction tensile residual stress at the outer surface of about 580 MPa, due to an autofrettage procedure. The notch and residual stress combined to produce a yield strength level sustained tensile stress at the notch roots.

Sustained yield strength level stress alone could not have caused the failure of the A723 (ASTM specification) steel used for the tube. The steel had considerable fracture toughness, as indicated by the values of V-notched Charpy impact energy and fracture toughness in Table 2. It was the aggressive warm acid environment (see Table 2) combined with the sustained tensile stress that caused the failure. The sulfuric and phosphoric acid mixture at 54°C was used for electropolishing the steel before plating. Environmentally-assisted cracking was found to occur in this acid environment at values of applied K as low as about 20 MPa$\sqrt{m}$ in the tests described earlier in relation to Figure 3. This is only one-sixteenth of the value of fracture toughness--the applied K at which cracking is expected in response to a single or sustained load without assistance from an aggressive environment.

As a result of the investigation, it was recommended to prevent or minimize contact of the acid with the notch root, if practical, or to significantly increase the notch root radius in order to reduce the value of sustained tensile stress.

Table 2 - Summary of Analysis of Environmental Cracking of NiCrMo Steel Cannon Tube with Tensile Residual Stress and Subjected to Acid Environment

Results of Mechanical Tests					
Yield Strength	Charpy Energy	Fracture Toughness	Environmentally-Assisted Cracking Tests		
			K_0	Exposure Time	K_{Ieac}
1207 MPa	28 J	157 MPa√m	110 MPa√m	1600 hours	18 MPa√m
			82 MPa√m	1550 hours	19 MPa√m
			54 MPa√m	1550 hours	16 MPa√m

Characterization of Environment		
Concentrated H_2SO_4 (98% by weight)	Concentrated H_3PO_4 (85% by weight)	Test Temperature
50% by volume	50% by volume	54°C

FAST FRACTURE OF CARBON/EPOXY COMPOSITE LAMINATES

Generally, composite laminates can be divided into two categories: interlaminar fracture involving delamination between plies and translaminar fracture involving through-thickness fracture often induced by external through-thickness damage. Delamination fracture tests and analysis have been well addressed, as shown for example, by a series of ASTM symposia and proceedings, the latest of which is Reference 8. Translaminar fracture is less likely to occur in most composite laminates, and therefore has not been addressed as much. The important work of Harris and Morris (ref 9) shows how to proceed with translaminar fracture testing and analysis of laminates and gives results for several types of carbon/epoxy laminates.

The current author and coworkers have investigated the translaminar fracture of composite laminates to develop standard methods of test and analysis. Comparisons of the mechanical load-displacement behavior with the notch-tip damage behavior were made with one type of quasi-isotropic carbon/epoxy laminate (ref 10). An interlaboratory program of fracture tests and associated damage characterization of various types of carbon/epoxy laminates in three test configurations was described in more recent work (ref 11). The remainder of this report reviews some of this recent work (ref 11), which was based on the approach of References 9 and 10 and was directed at the development of a translaminar fracture toughness test procedure for carbon/epoxy laminates.

4

Test Configurations, Stress Analyses

The initial plan in the translaminar fracture tests of laminates was to use the compact and three-point bend specimens for the tests--the same configurations used for a variety of fracture tests for metals. As the work progressed, problems arose with the compact and three-point bend specimens for use with laminates, as discussed later. This led to the use of a third specimen configuration, called the extended compact, see Figure 6. This type of specimen has been used recently by Piascik and Newman (ref 12), who obtained numerical values of K/P and V/P versus a/W for this configuration, which are required for analysis of fracture tests. Wide range expressions for K/P and V/P were developed (ref 11) and are compared with the numerical results in Figure 7. The expressions, given below, include the functional form of the shallow and deep crack limit solutions (ref 13), and they fit both the numerical results and the limits within one percent.

$$KBW^{1/2}/P = \alpha^{1/2}[1.4+\alpha][3.97-10.88\,\alpha+26.25\,\alpha^2-38.9\,\alpha^3+30.15\,\alpha^4-9.27\,\alpha^5]/[1-a]^{3/2} \quad (1)$$
$$for\ 0 \le \alpha \le 1 \ ; \ \alpha = a/W$$

$$VEB/P = [15.52\,\alpha-26.38\,\alpha^2+49.70\,\alpha^3-40.74\,\alpha^4+14.44\,\alpha^5]/[1-\alpha]^2 \quad (2)$$
$$for\ 0 \le \alpha \le 1$$

The inverse of Eq. (2) that fits it within 0.04 percent is

$$\alpha = 1.0004 - 3.5495\,u + 6.0988\,u^2 - 16.0075\,u^3 + 32.3436\,u^4 - 22.2843\,u^5 \quad (3)$$
$$for\ u = 1/[(VEB/P)^{1/2} + 1] \ , \ 0.15 \le \alpha \le 1$$

Equations (1) through (3) were used to obtain K, V, a/W, and elastic modulus, E, values from the P-V plots, as described in the upcoming discussion of fracture test results.

Another type of stress analysis result that is important when performing fracture tests with composite laminates is the nominal bending stresses controlling crack direction in the various test configurations. The damage ahead of the notch tip can occur in such a way that the crack growth direction is normal to the notch axis rather than parallel to it as intended in the self-similar crack growth of a fracture test. In Reference 11, calculations of the nominal bending stress in two directions at the notch tip were made which showed why off-axis cracking can occur for some combinations of laminate layup and specimen configuration. The results of these calculations are summarized in Figure 8 for each of the three test configurations. The calculations of S_Y and S_X, the nominal, notch-tip bending stresses that control self-similar and off-axis cracking, respectively, for the extended compact specimen are as follows, referring also to Figure 8. The expression

$$S_Y = 6M/B(W-a)^2 \quad (4)$$

gives the y-direction nominal bending stress that drives self-similar cracking from the notch, where the applied moment, M, is

$$M = 6P[a-0.2W+(W-a)/2] \quad (5)$$

5

Combining Eqs. (4), (5), and (1) gives

$$S_Y W^{1/2}/K = 3(1+0.6\alpha)/f_E(1-\alpha)^2 \qquad (6)$$

where $f_E = KBW^{1/2}/P$, from Eq. (1). For the x-direction bending stress that drives off-axis cracking in the extended compact specimen

$$S_x = 6M/BH^2 \qquad (7)$$

and

$$M = 6P(\alpha - 0.2W) \qquad (8)$$

and the result is

$$S_x W^{1/2}/K = 16.67(\alpha - 0.2)/f_E \qquad (9)$$

Equations (6) and (9) are plotted in Figure 8, along with the comparable expressions for the standard compact and bend specimens. They compare the bending stresses that control self-similar and off-axis cracking for the three specimen configurations. The plot of $SW^{1/2}/K$ provides a dimensionless comparison of these important bending stresses at any given applied K level and for a range of a/W. For the standard compact specimen at relatively small a/W, the off-axis bending stress approaches the same magnitude as that for self-similar cracking. This explains the off-axis cracking problems with this specimen that are described in the upcoming results. Note that this problem is not expected for the extended compact specimen or for the three-point bend specimen. The large dimensions of these specimen configurations in the direction perpendicular to the notch reduces the bending stress, S_x, that drives off-axis cracking so that this type of cracking does not occur.

Fracture Test Results with Laminates

The materials tested in the recent work (ref 11) were T300 carbon fiber/976 epoxy and AS4 carbon fiber/977-2 toughened epoxy in various symmetrical layups shown in Table 3. The [0/+45/90/-45] and [90/-45/0/+45] layups were selected because of the common usage of quasi-isotropic laminates in composite structures. The [0/0/90] and [90/90/0] layups were selected to investigate the problems that can arise in fracture testing of materials with considerable orthotropy. Problems became immediately apparent in the P-V tests, as shown by the elastic modulus determined from the slope. Note in Table 3 that the modulus for the [0/0/90] layup standard compact specimen of both materials was lower than expected due to the tendency toward off-axis cracking discussed earlier. Many [0/0/90] samples, particularly of the more brittle T300/976 material, showed complete off-axis failure. Essentially, one of the loading arms broke off. This behavior eliminates the standard compact configuration as a generally useful specimen in translaminar fracture tests of laminates, because laminate is often used with this much orthotropy.

6

Table 3 - Test Conditions and Elastic Modulus Results

Material/Thickness	Modulus, E(GPa), From Measured P-V Slope		
	Three-Point Bend	Standard Compact	Extended Compact
T300/976 Laminates			
[0/+45/90/-45]$_{4s}$, 2.1 mm	54	57	55
[90/-45/0/+45]$_{4s}$, 2.1 mm	47*	55	59
[0/0/90]$_{6s}$, 2.4 mm	47	37*	45
[90/90/0]$_{6s}$, 2.4 mm	33	32	34
AS4/977-2 Laminates			
[0/+45/90/-45]$_{4s}$, 4.2 mm	52	60	53
[90/-45/0/+45]$_{4s}$, 4.2 mm	55	58	56
[0/0/90]$_{6s}$, 4.8 mm	45	30*	44
[90/90/0]$_{6s}$, 4.8 mm	32	29	34

*Lower than expected

The other lower than expected modulus noted in Table 3 also had an important implication. Compressive failure could be seen with the unaided eye around the center load point for some of the [90/-45/0/+45] layup bend specimens. This load-point failure can affect fracture behavior as well as modulus, so the three-point bend specimen is also eliminated as a generally useful test configuration. This led to interest in the extended compact specimen with $H/W = 1.9$, as mentioned earlier. This specimen is not prone to off-axis cracking, as shown by the results in Figure 8 and has no load point ahead of the notch, so it will not be subject to the arm breaking and load-point problems discussed above.

Typical P-V plots are shown in Figure 9. Note the initial linear slope used for modulus determination and the deviation from the linear line, ΔV compared to V_o. By using Eqs. (2) and (3), the crack growth associated with ΔV can be calculated and used to determine the applied K value at maximum load, K_{max}. Comparisons of the relative crack growth, $\Delta(a/W)$, determined from ΔV with those from the unloading slope and from radiographic damage measurements are shown in Figure 10. For tests of various layups of both materials and each of the three specimen configurations, the values of crack growth agree closely, so it is believed to be appropriate to use

the crack growth to calculate K_{max}. Note also that the amount of crack growth by either method corresponds to about 80 percent of the apparent Δa determined from the radiographs. Apparently, the damage near the outer extent of the zone identified by radiography is not severe enough to correspond to effective crack growth. Another explanation for why the calculated Δa is less than the extent of the radiographic damage zone is that fiber bridging occurs and increases the stiffness of the cracked specimen as if Δa were smaller.

The overall trend of the K_{max} results, as well as the crack growth results from the laminate tests, can be seen in a plot of K_{max} versus the calculated amount of crack growth at K_{max} (see Figure 11). The quasi-isotropic layups of both materials show indications of increasing resistance to crack growth, that is, an increasing K-R curve. This is consistent with the fact that most fibers in these layups can bridge the crack and pull out as the crack grows, and thereby provide increasing crack growth resistance. The AS4 [90/90/0] layup shows no increasing K-R behavior, as would be expected, since most of its fibers can not bridge the crack. The AS4 [0/0/90] results for the standard compact and bend specimens, indicated by C and B, respectively, are suspect for the reasons discussed earlier. The AS4 [0/0/90] results for the extended compact are more likely to be correct, and their K_{max} value is nearly three times that of the AS4 [90/90/0] results, as would be expected based on the relative amounts of 0-degree fibers in each layup.

The following is the method proposed for translaminar fracture toughness determination based on these tests of carbon/epoxy laminates. The extended compact specimen is used, the P versus V plot is recorded, and K_{max} is calculated taking into account the crack growth determined from ΔV. K_{max} gives a good measure of fracture toughness provided that $\Delta V/V_o \leq 0.3$ based on the results in Figure 11. This method of fracture toughness would give consistent results, and the $\Delta V/V_o \leq 0.3$ criterion would exclude tests with large amounts of damage and cracking extending perpendicular to the notch, such as for tests of layups with a significant portion of 0-degree fibers.

CONCLUSIONS

Fracture Tests with Steels

Three fracture test and analysis methods were described that provide good descriptions of fracture in armament components. The compliance unloading J_{Ic} fracture toughness test was described in a failure analysis of a stainless steel welded structure. The three-point bend configuration can now be used with a single, direct displacement measurement at the crack mouth that gives crack growth measurement throughout the test. The $K/\sqrt{r}$ fatigue initiation analysis gave a good description of the measured fatigue initiation lives for bend specimens of four different weld and plate samples of high strength stainless steel. By using the ratio of the maximum notch root stress to material yield strength, an S-N plot of results from four different materials gives a single trend line that can be used quite generally for descriptions of fatigue initiation life of structures. Test and analysis methods for describing environmentally-assisted cracking were explained using the bolt-loaded compact test configuration to address environmental cracking in a nickel-chromium-molybdenum high strength steel. The bolt-loaded test is both simple and portable, and an accurate, wide range K expression is now available for this test configuration.

8

Failure of a welded stainless steel beam emphasized the importance of the proper heat treated condition for obtaining high fracture toughness and high fatigue life. Omission of the solution heat treatment resulted in the lowest J_{Ic} value, the lowest J-R curve, and the lowest fatigue initiation lives.

An unanticipated failure of a cannon tube during a plating process showed that when the basic requirements for environmentally-assisted cracking are present, loading and material conditions normally considered safe can be brushed aside. Even though the tube had good inert environment fracture toughness and no external loads, a complete structural failure occurred due to the presence of a notch, a tensile residual stress, and an aggressive acid environment.

Fracture Tests with Composite Laminates

Fracture tests were performed with carbon/polymer laminates and analyzed to develop translaminar fracture toughness test and analysis procedures. Notched specimens of four symmetrical layups were tested: [0/+45/90/-45], [90/-45/0/+45], [0/0/90], and [90/90/0]; two carbon fiber/epoxy materials: a relatively brittle T300 fiber/976 epoxy and a tougher AS4 fiber/977-2 epoxy; and three specimen configurations: the standard three-point bend and compact configurations used for many types of fracture tests, and an extended compact specimen with arm-height to specimen-width ratio of 1.9, compared to 0.6 for the standard compact specimen. Plots of load versus crack mouth opening displacement were obtained and analyzed to determine the progression of crack growth and damage during the test.

Wide range stress and displacement expressions were obtained for the extended compact specimen. Expressions for applied stress intensity factor, K, and crack mouth opening displacement, V, in terms of relative notch length, a/W, and for a/W in terms of V were developed from recent numerical results. Relationships for the nominal bending stresses that control both self-similar and off-axis cracking for the extended compact specimen were derived and used to explain the types of cracking observed.

Damage unrelated to crack growth from the notch tip was characterized in the tests, including the damage associated with the arm breakage problem with the standard compact specimen, and the load-point damage with the three-point bend specimen. Notch-tip damage was characterized using radiography, and the extent of the radiographic damage zone ahead of the notch tip compared well with elastic calculations of crack growth.

The applied K at maximum load, K_{max}, including the effect of the crack growth up to the maximum load point, was used as a measure of fracture toughness. Plots of K_{max} versus crack growth showed an increasing resistance to crack growth for quasi-isotropic layups and a constant resistance to crack growth for predominantly 90-degree fiber layups. The K_{max} from the extended compact specimen, including the effect of crack growth, was proposed as a measurement of translaminar fracture toughness for carbon/epoxy laminates. For relatively small deviations from the linear extension of the P-V plot, the K_{max} values gave consistent measurements of fracture toughness. This criterion also excluded tests with significant damage other than at the notch tip--damage that can violate the concept of fracture toughness measurement.

9

REFERENCES

1. *Elastic-Plastic Fracture Test Methods: The User's Experience (Second Volume), ASTM STP 1114*, J.A. Joyce, Ed., American Society for Testing and Materials, Philadelphia, 1991.

2. J.M. Barsom and S.T. Rolfe, *Fracture and Fatigue Control in Structures*, Prentice-Hall, Englewood Cliffs, NJ, 1987.

3. R.P. Wei and S.R. Novak, *Journal of Testing and Evaluation*, Vol. 15, No. 1, January 1987, pp. 38-75.

4. J.H. Underwood, R.A. Farrara, G.P. O'Hara, J.J. Zalinka, and J. Senick, in: *Elastic-Plastic Fracture Test Methods: The User's Experience (Second Volume), ASTM STP 1114*, J.A. Joyce, Ed., American Society for Testing and Materials, Philadelphia, 1991, pp. 197-212.

5. M.T. Kirk and R.H. Dodds, Jr., *Journal of Testing and Evaluation*, Vol. 21, No. 4, June 1993, pp. 228-238.

6. J.H. Underwood, E.J. Troiano, and R.T. Abbott, *Fracture Mechanics: Twenty-Fourth Symposium, ASTM STP 1207*, American Society for Testing and Materials, Philadelphia, 1995.

7. J.H. Underwood, V.J. Olmstead, J.C. Askew, A.A. Kapusta, and G.A. Young, *Fracture Mechanics: Twenty-Third Symposium, ASTM STP 1189*, American Society for Testing and Materials, Philadelphia, 1993, pp. 443-460.

8. *Composite Materials: Fourth Volume, ASTM STP 1156*, W.W. Stinchcomb and N.E. Ashbaugh, Eds., American Society for Testing and Materials, Philadelphia, 1993.

9. C.E. Harris and D.H. Morris, *Fracture Mechanics: Seventeenth Volume, ASTM STP 905*, American Society for Testing and Materials, Philadelphia, 1986, pp. 124-135.

10. J.H. Underwood and M.T. Kortschot, *Proceedings of the Second International Conference on Deformation and Fracture of Composites*, The Institute of Materials, London, 1993.

11. J.H. Underwood, M.T. Kortschot, W.R. Lloyd, H.L. Eidinoff, D.A. Wilson, and N. Ashbaugh, *Fracture Mechanics: 26th Volume, ASTM STP 1256*, American Society for Testing and Materials, Philadelphia, 1995.

12. R.S. Piascik and J.C. Newman, *International Journal of Fracture*, to be published.

13. H. Tada, P.C. Paris, and G.R. Irwin, *The Stress Analysis of Cracks Handbook*, Paris Productions, St. Louis, MO, 1985.
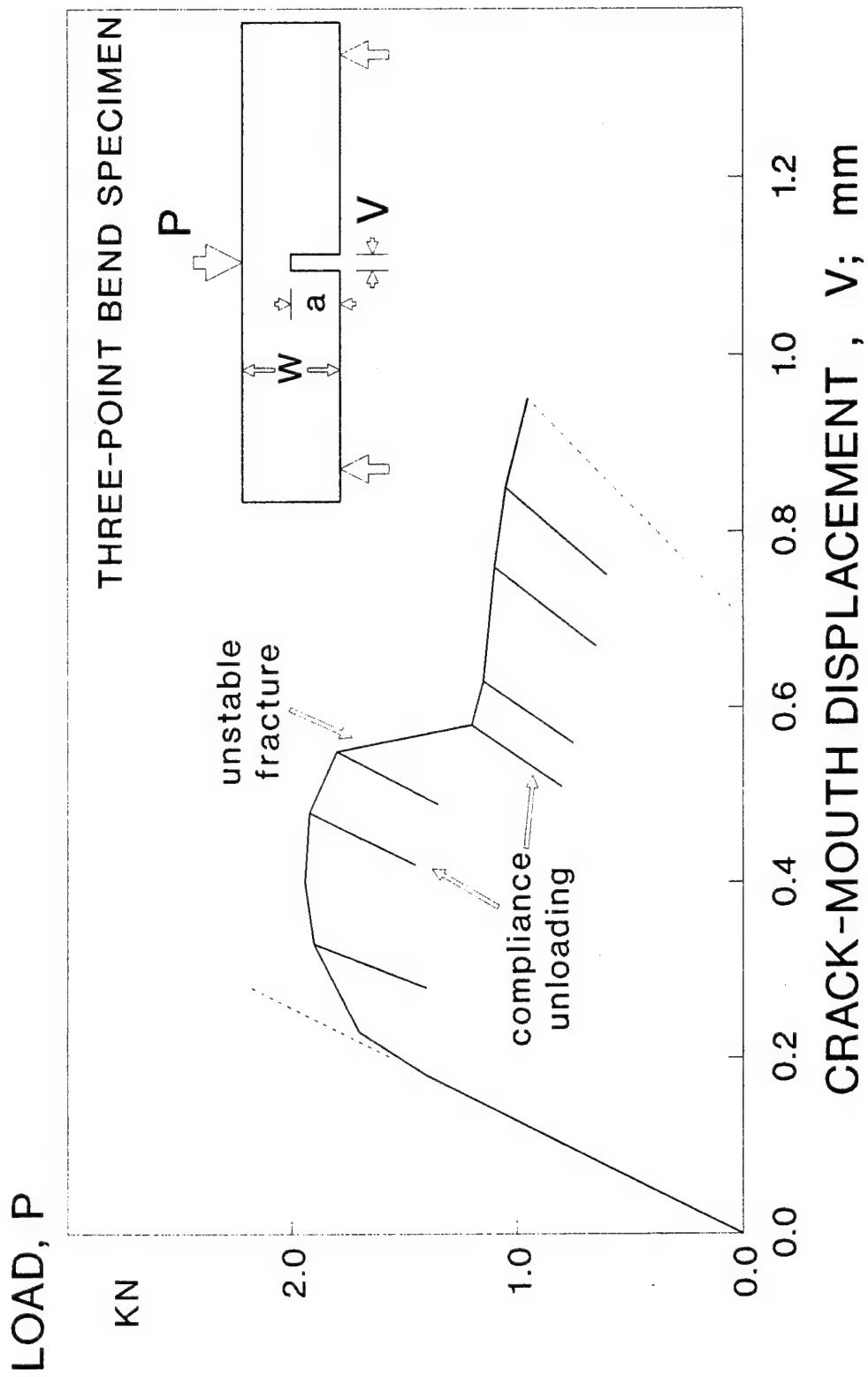
FIGURE 1
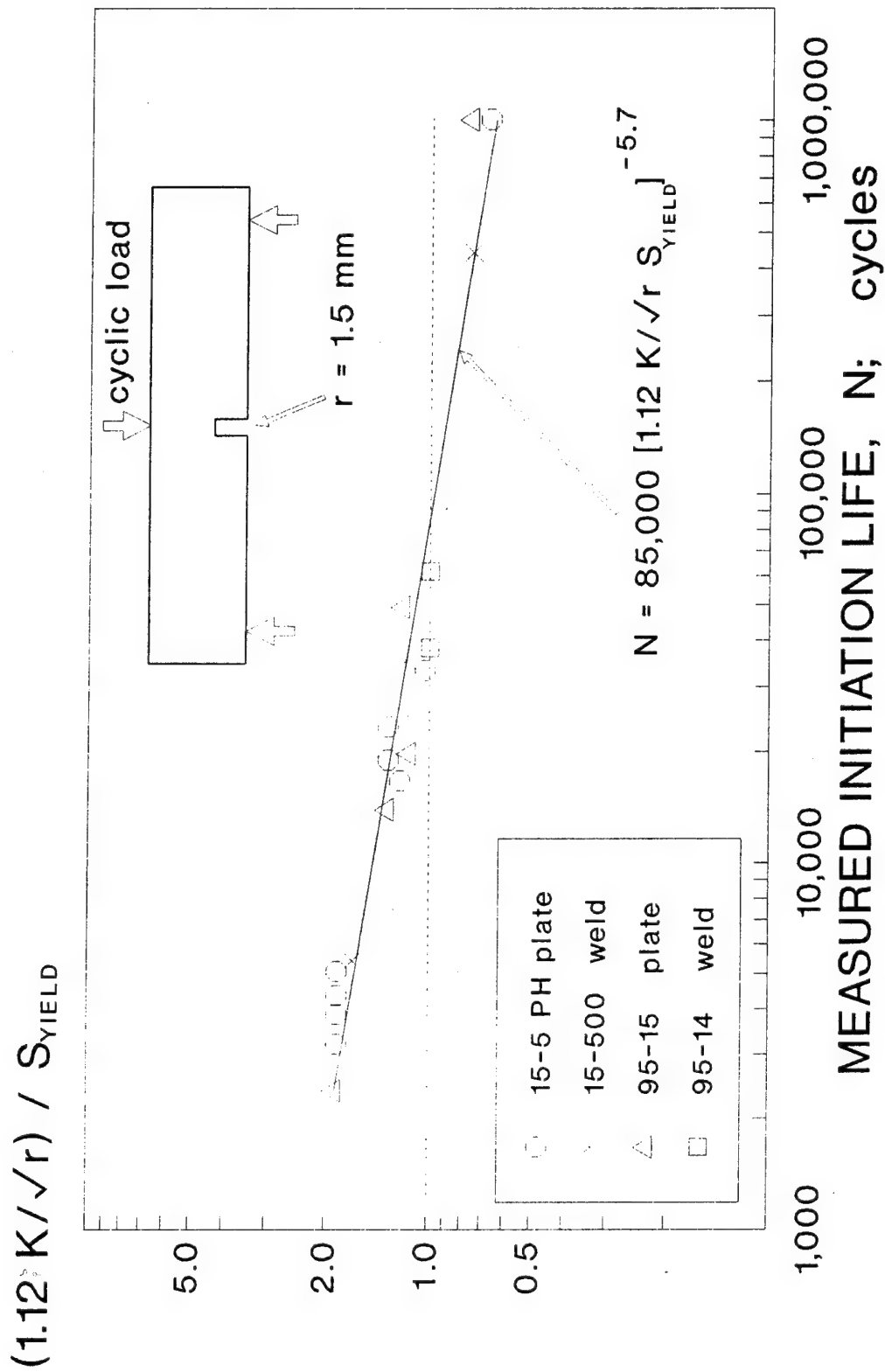J_{Ic} test of 15-500 PH stainless steel weld; welded and aged at 593 C

11

FIGURE 2
Fatigue life tests and analysis of
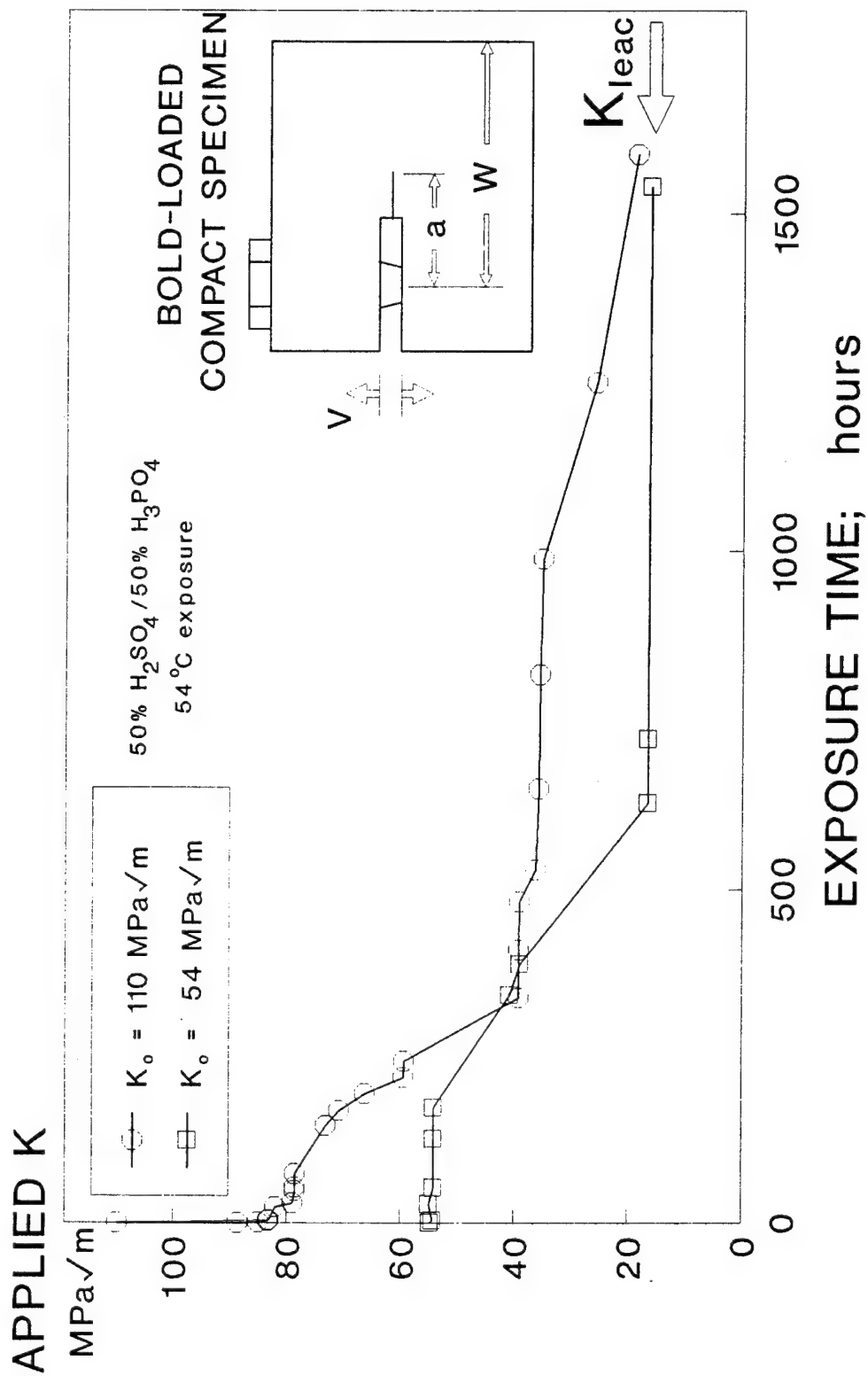PH stainless steel welds and plate

12

FIGURE 3
K_{Ieac} *tests of 1210 MPa yield strength*
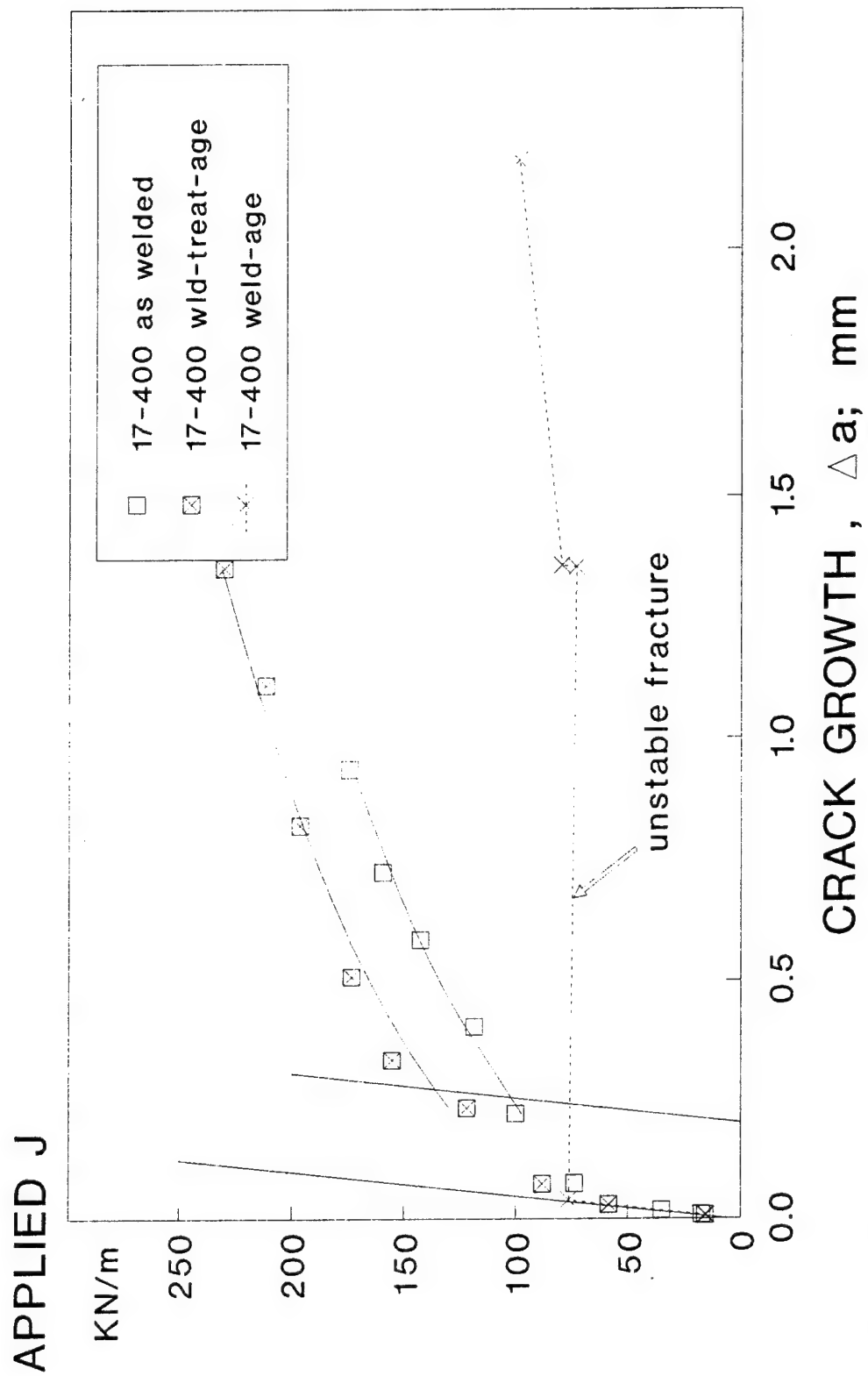*NiCrMo steel in acid environment*

13

FIGURE 4
J_{Ic} tests of 17-400 PH stainless steel
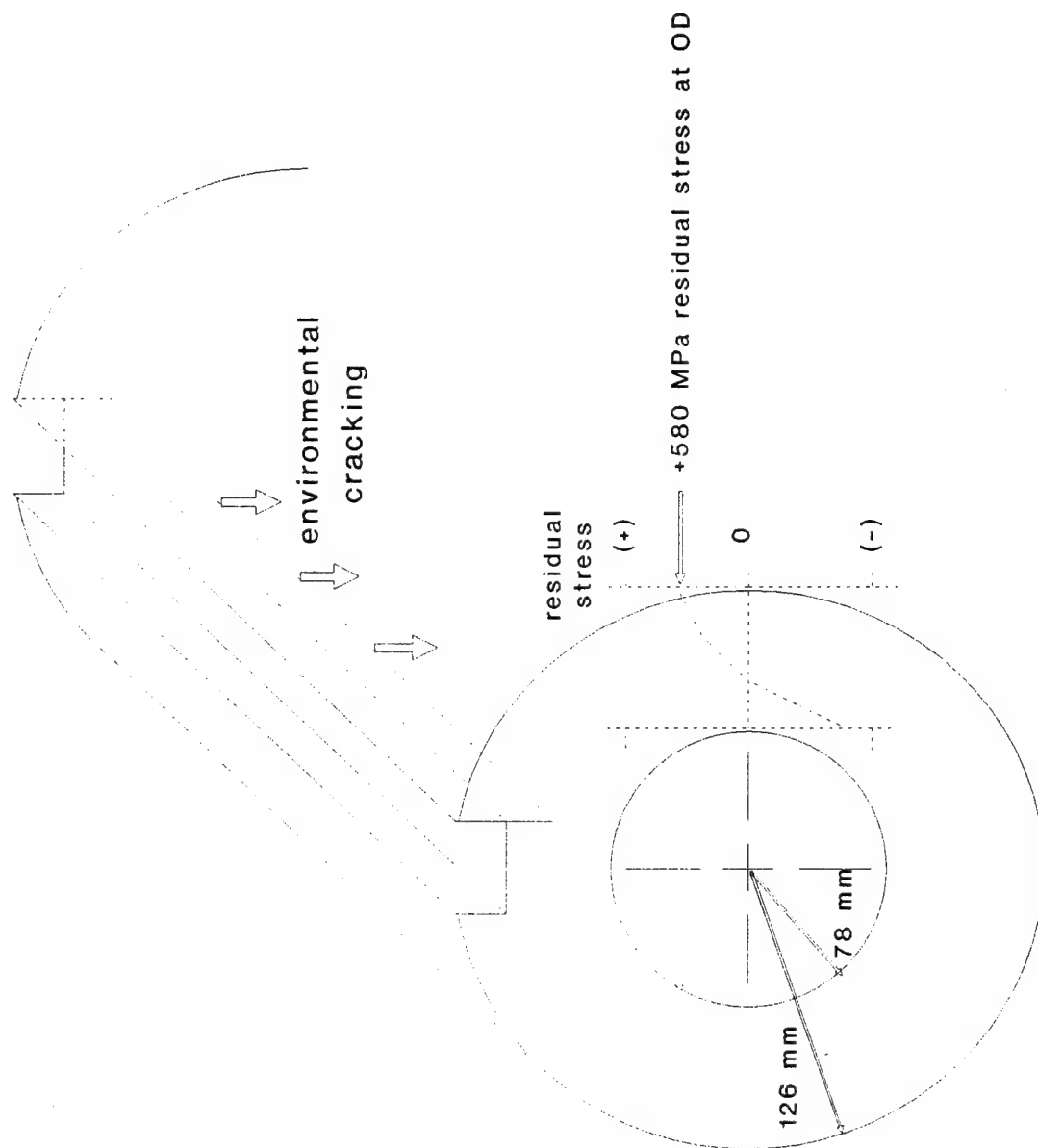welds with various heat treatments

14

FIGURE 5
Environmental cracking at an OD notch in
a cannon with tensile residual stress

residual
stress

(+)

0

(−)

+580 MPa residual stress at OD

environmental
cracking

78 mm

126 mm

THREE-POINT BEND

W; 25.0

a

110 mm

55 mm

EXTENDED COMPACT; H/W = 1.9

5.0 dia

5.0

37.5

a

95 mm

H

W; 25.0
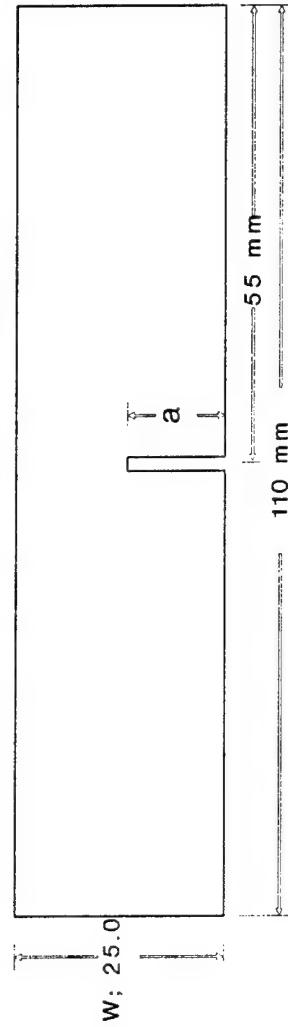
STANDARD COMPACT; H/W = 0.6

31.25 mm

a

H 7.0
30.0 mm

W; 25.0

5.0 dia
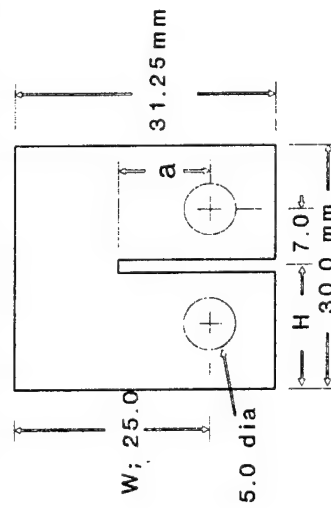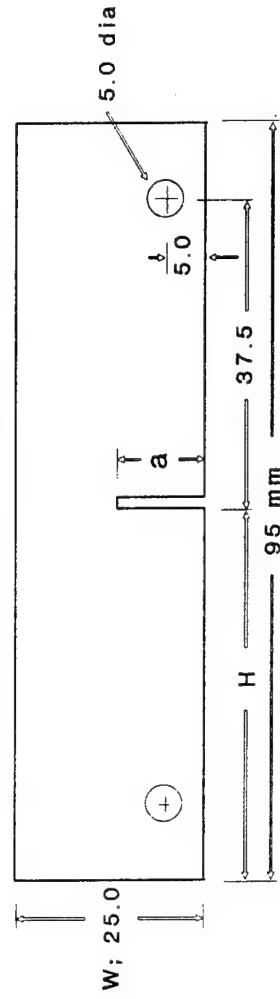
FIGURE 6

Specimen configurations for translaminar fracture tests with composite laminates

16

K and V
results
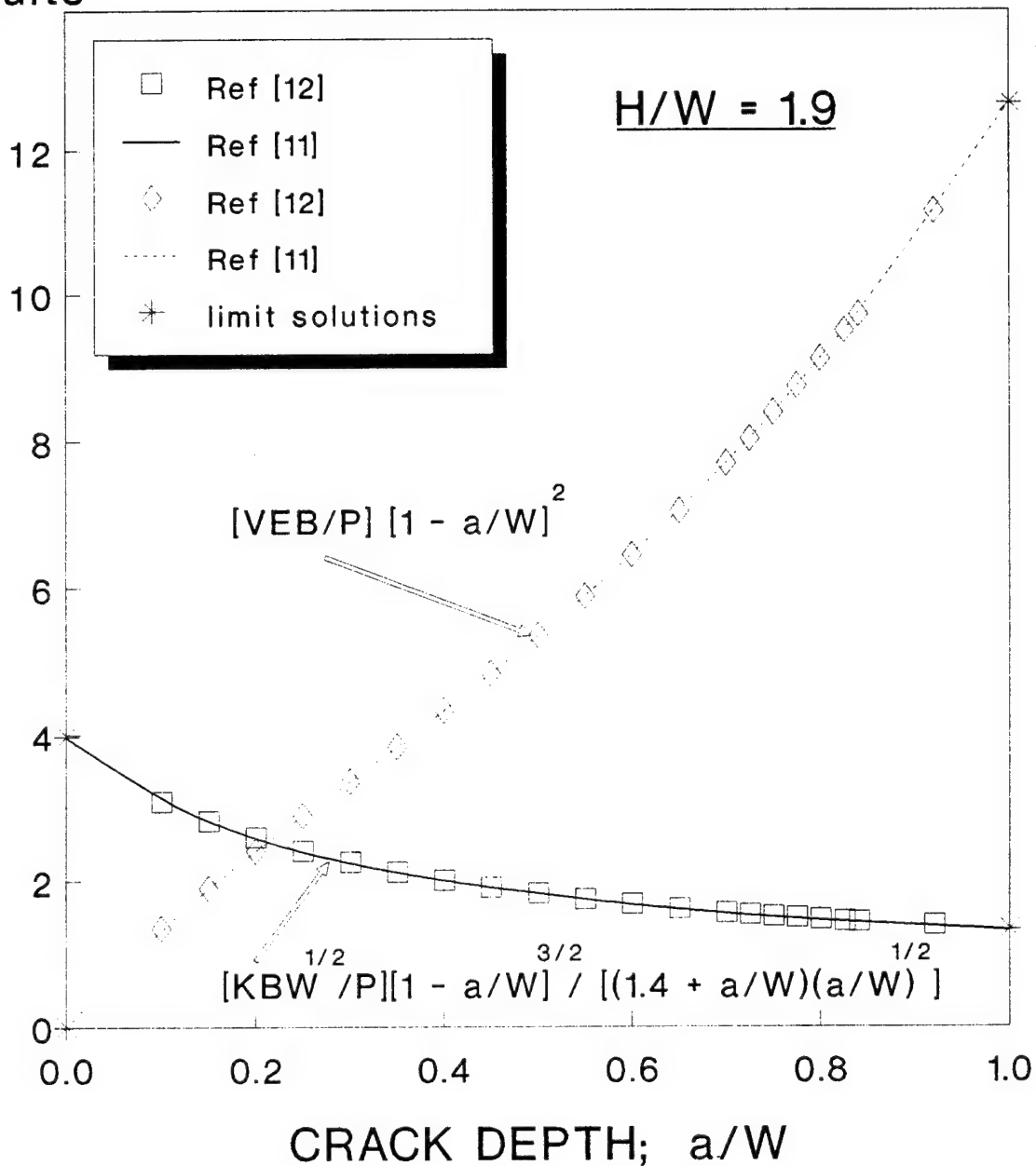
FIGURE 7
Stress intensity & displacement results
for the extended compact specimen

17

FIGURE 8
Bend stresses controling crack direction
in three fracture test specimens

18

FIGURE 9
Load vs V for three specimen types;
T300/976 with [90/-45/0/45] layup

19
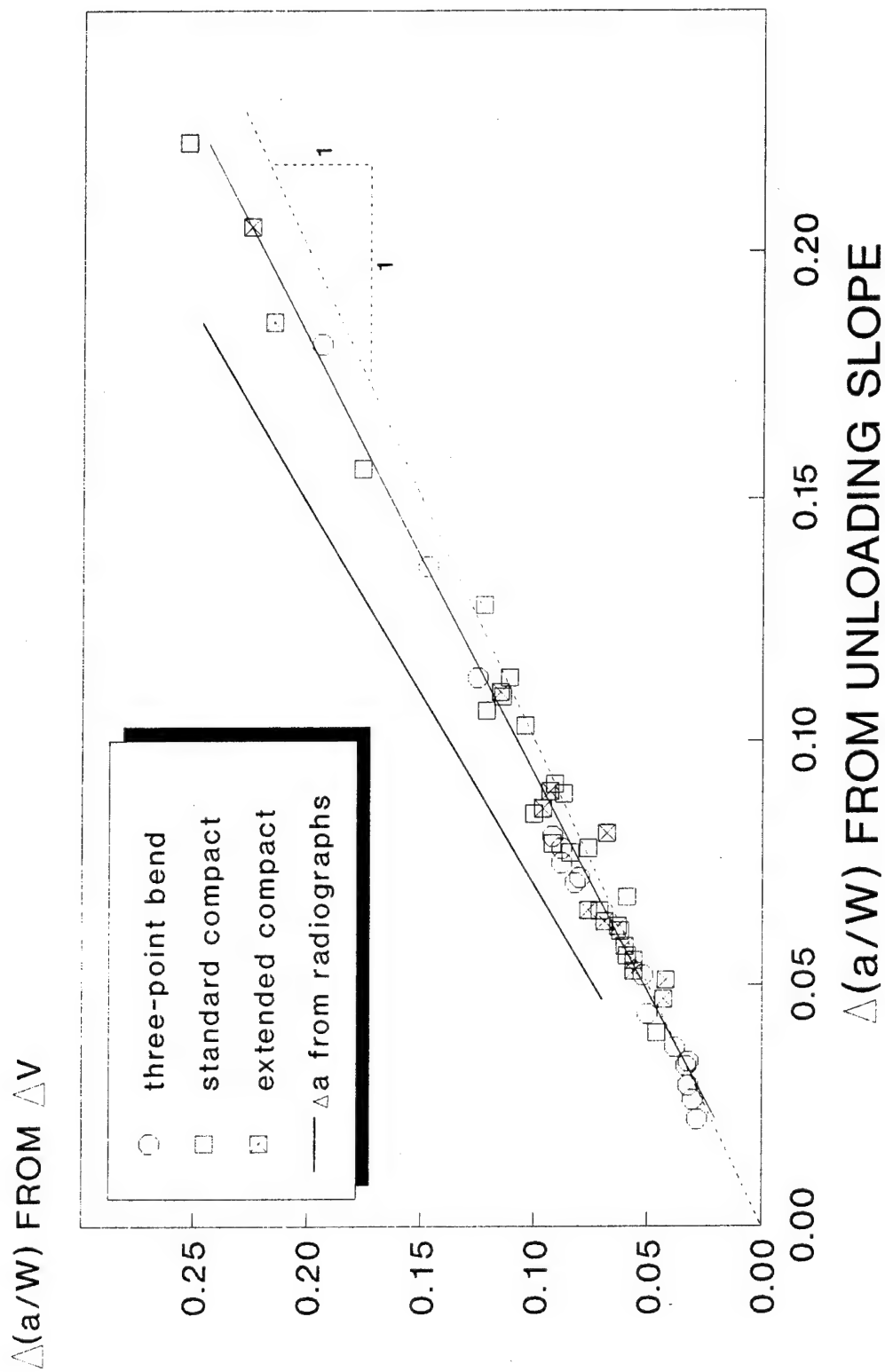
FIGURE 10
Load vs V calculations of crack growth
compared with radiographic measurements

20
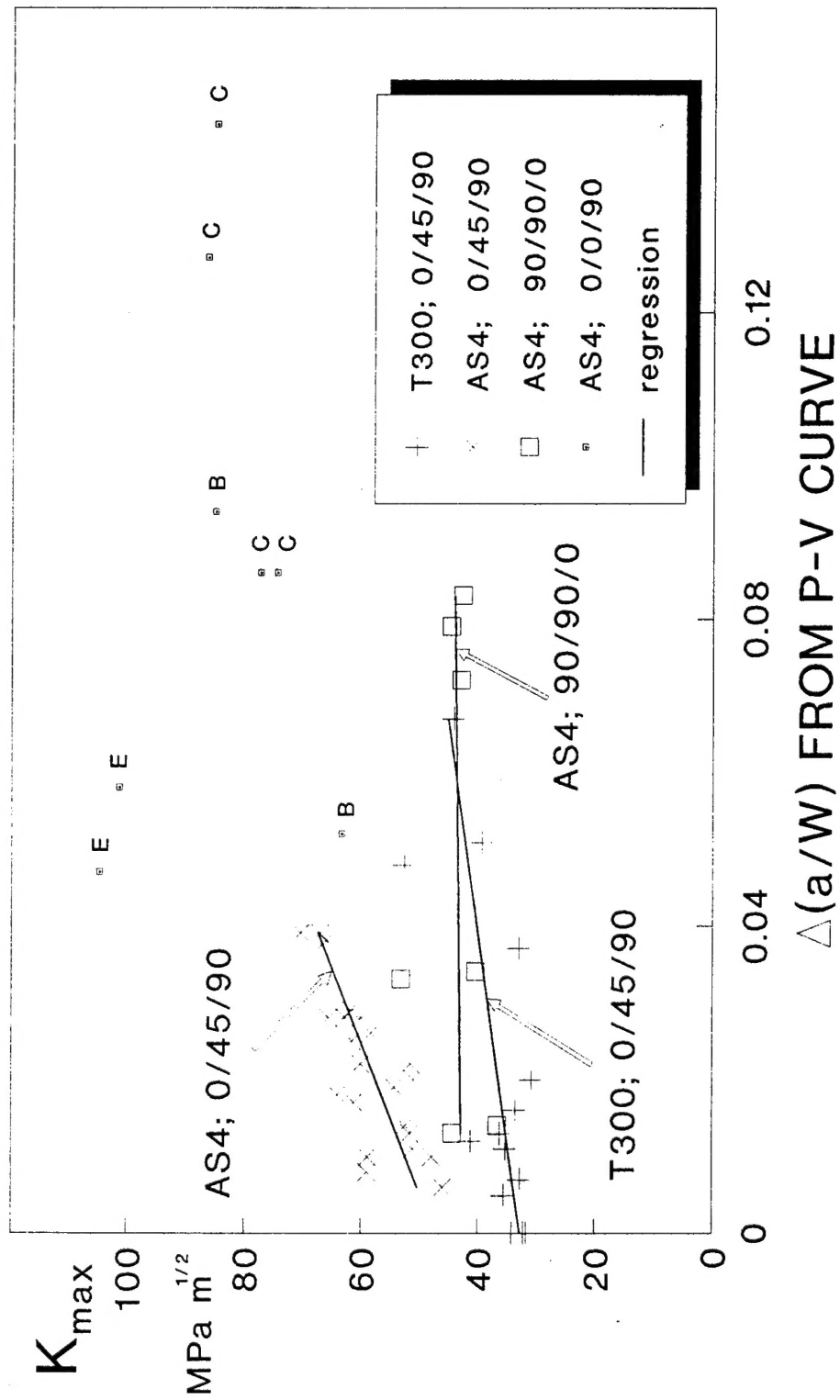
FIGURE 11
Applied K and crack growth at point of
maximum load for various laminates

21

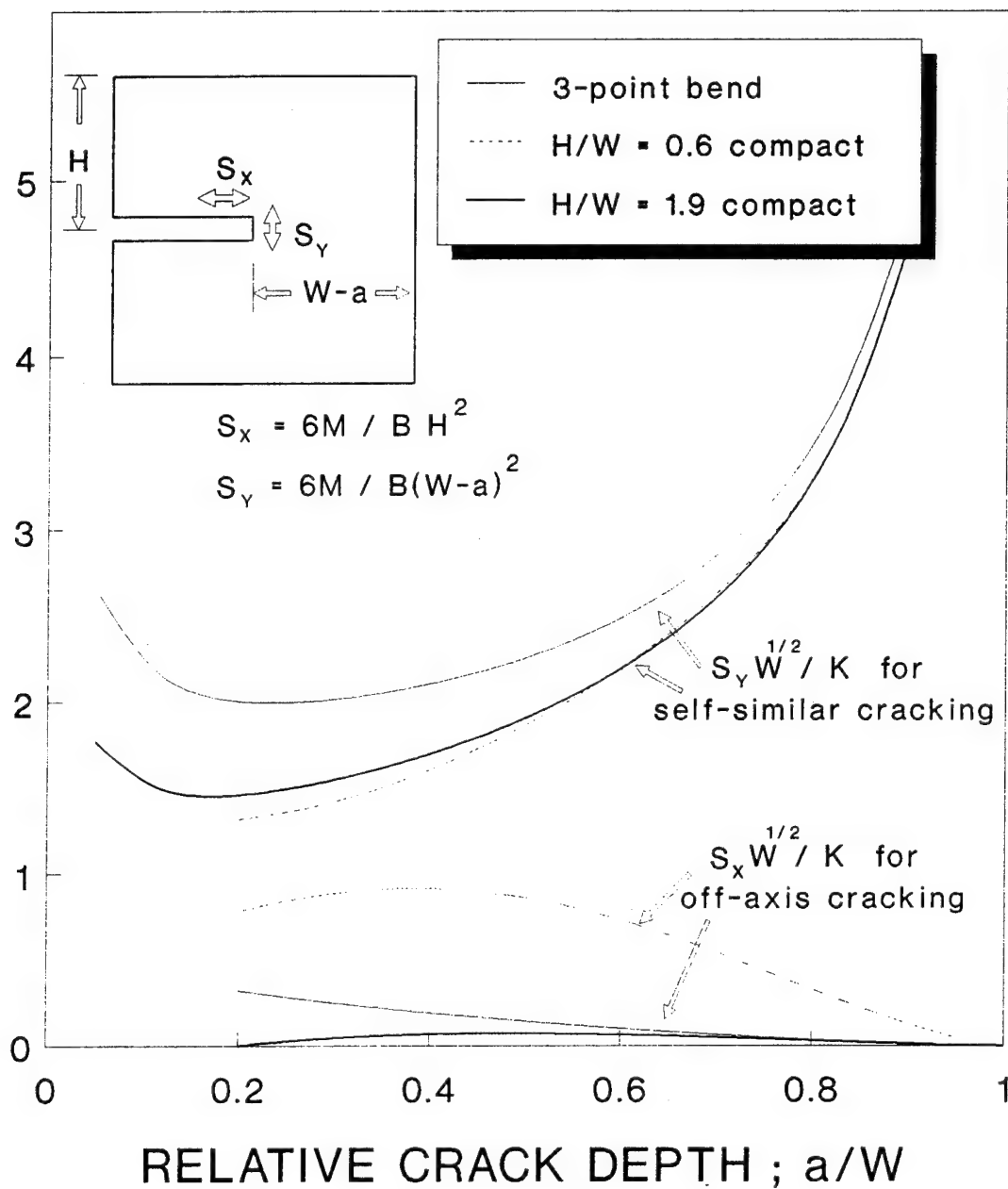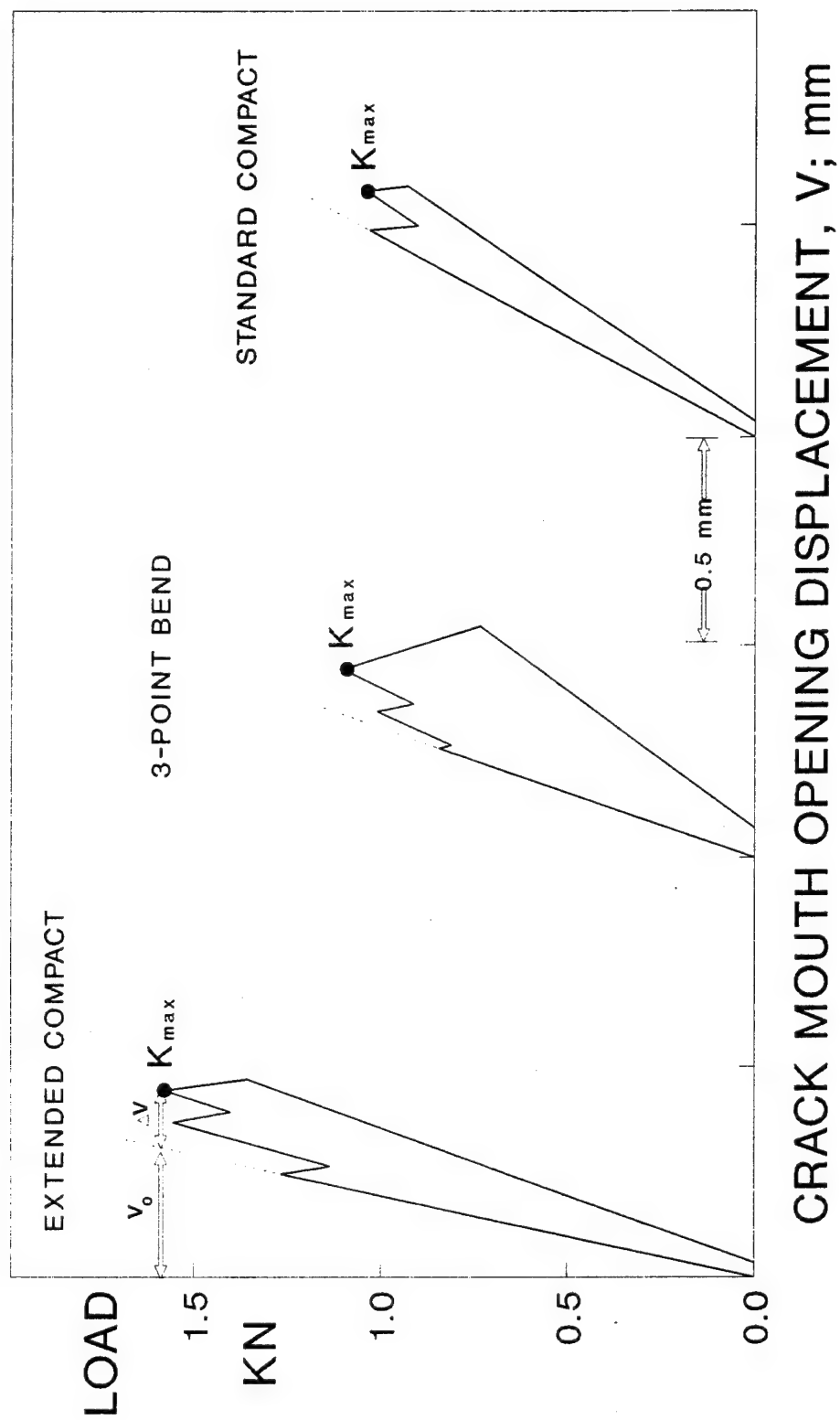# TECHNICAL REPORT INTERNAL DISTRIBUTION LIST

	NO. OF COPIES
CHIEF, DEVELOPMENT ENGINEERING DIVISION	
ATTN: AMSTA-AR-CCB-DA	1
-DB	1
-DC	1
-DD	1
-DE	1
CHIEF, ENGINEERING DIVISION	
ATTN: AMSTA-AR-CCB-E	1
-EA	1
-EB	1
-EC	
CHIEF, TECHNOLOGY DIVISION	
ATTN: AMSTA-AR-CCB-T	2
-TA	1
-TB	1
-TC	1
TECHNICAL LIBRARY	
ATTN: AMSTA-AR-CCB-O	5
TECHNICAL PUBLICATIONS & EDITING SECTION	
ATTN: AMSTA-AR-CCB-O	3
OPERATIONS DIRECTORATE	
ATTN: SMCWV-ODP-P	1
DIRECTOR, PROCUREMENT & CONTRACTING DIRECTORATE	
ATTN: SMCWV-PP	1
DIRECTOR, PRODUCT ASSURANCE & TEST DIRECTORATE	
ATTN: SMCWV-QA	1

NOTE: PLEASE NOTIFY DIRECTOR, BENÉT LABORATORIES, ATTN: AMSTA-AR-CCB-O OF ADDRESS CHANGES.

TECHNICAL REPORT EXTERNAL DISTRIBUTION LIST

	NO. OF COPIES		NO. OF COPIES
ASST SEC OF THE ARMY RESEARCH AND DEVELOPMENT ATTN: DEPT FOR SCI AND TECH THE PENTAGON WASHINGTON, D.C. 20310-0103	1	COMMANDER ROCK ISLAND ARSENAL ATTN: SMCRI-ENM ROCK ISLAND, IL 61299-5000	1
ADMINISTRATOR DEFENSE TECHNICAL INFO CENTER ATTN: DTIC-OCP (ACQUISITION GROUP) BLDG. 5, CAMERON STATION ALEXANDRIA, VA 22304-6145	2	MIAC/CINDAS PURDUE UNIVERSITY P.O. BOX 2634 WEST LAFAYETTE, IN 47906	1
COMMANDER U.S. ARMY ARDEC ATTN: SMCAR-AEE	1	COMMANDER U.S. ARMY TANK-AUTMV R&D COMMAND ATTN: AMSTA-DDL (TECH LIBRARY) WARREN, MI 48397-5000	1

ASST SEC OF THE ARMY
RESEARCH AND DEVELOPMENT
ATTN: DEPT FOR SCI AND TECH   1
THE PENTAGON
WASHINGTON, D.C. 20310-0103

ADMINISTRATOR
DEFENSE TECHNICAL INFO CENTER   2
ATTN: DTIC-OCP (ACQUISITION GROUP)
BLDG. 5, CAMERON STATION
ALEXANDRIA, VA 22304-6145

COMMANDER
U.S. ARMY ARDEC
ATTN: SMCAR-AEE   1
        SMCAR-AES, BLDG. 321   1
        SMCAR-AET-O, BLDG. 351N   1
        SMCAR-FSA   1
        SMCAR-FSM-E   1
        SMCAR-FSS-D, BLDG. 94   1
        SMCAR-IMI-I, (STINFO) BLDG. 59   2
PICATINNY ARSENAL, NJ 07806-5000

DIRECTOR
U.S. ARMY RESEARCH LABORATORY
ATTN: AMSRL-DD-T, BLDG. 305   1
ABERDEEN PROVING GROUND, MD
     21005-5066

DIRECTOR
U.S. ARMY RESEARCH LABORATORY
ATTN: AMSRL-WT-PD (DR. B. BURNS)   1
ABERDEEN PROVING GROUND, MD
     21005-5066

DIRECTOR
U.S. MATERIEL SYSTEMS ANALYSIS ACTV
ATTN: AMXSY-MP   1
ABERDEEN PROVING GROUND, MD
     21005-5071

COMMANDER
ROCK ISLAND ARSENAL
ATTN: SMCRI-ENM   1
ROCK ISLAND, IL 61299-5000

MIAC/CINDAS
PURDUE UNIVERSITY
P.O. BOX 2634   1
WEST LAFAYETTE, IN 47906

COMMANDER
U.S. ARMY TANK-AUTMV R&D COMMAND
ATTN: AMSTA-DDL (TECH LIBRARY)   1
WARREN, MI 48397-5000

COMMANDER
U.S. MILITARY ACADEMY
ATTN: DEPARTMENT OF MECHANICS   1
WEST POINT, NY 10966-1792

U.S. ARMY MISSILE COMMAND
REDSTONE SCIENTIFIC INFO CENTER   2
ATTN: DOCUMENTS SECTION, BLDG. 4484
REDSTONE ARSENAL, AL 35898-5241

COMMANDER
U.S. ARMY FOREIGN SCI & TECH CENTER
ATTN: DRXST-SD   1
220 7TH STREET, N.E.
CHARLOTTESVILLE, VA 22901

COMMANDER
U.S. ARMY LABCOM
MATERIALS TECHNOLOGY LABORATORY
ATTN: SLCMT-IML (TECH LIBRARY)   2
WATERTOWN, MA 02172-0001

COMMANDER
U.S. ARMY LABCOM, ISA
ATTN: SLCIS-IM-TL   1
2800 POWER MILL ROAD
ADELPHI, MD 20783-1145

NOTE: PLEASE NOTIFY COMMANDER, ARMAMENT RESEARCH, DEVELOPMENT, AND ENGINEERING CENTER,
          BENÉT LABORATORIES, CCAC, U.S. ARMY TANK-AUTOMOTIVE AND ARMAMENTS COMMAND,
          AMSTA-AR-CCB-O, WATERVLIET, NY 12189-4050 OF ADDRESS CHANGES.

	NO. OF COPIES		NO. OF COPIES
COMMANDER U.S. ARMY RESEARCH OFFICE ATTN: CHIEF, IPO P.O. BOX 12211 RESEARCH TRIANGLE PARK, NC 27709-2211	1	WRIGHT LABORATORY ARMAMENT DIRECTORATE ATTN: WL/MNM EGLIN AFB, FL 32542-6810	1
DIRECTOR U.S. NAVAL RESEARCH LABORATORY ATTN: MATERIALS SCI & TECH DIV CODE 26-27 (DOC LIBRARY) WASHINGTON, D.C. 20375	1 1	WRIGHT LABORATORY ARMAMENT DIRECTORATE ATTN: WL/MNMF EGLIN AFB, FL 32542-6810	1

NOTE: PLEASE NOTIFY COMMANDER, ARMAMENT RESEARCH, DEVELOPMENT, AND ENGINEERING CENTER,
     BENÉT LABORATORIES, CCAC, U.S. ARMY TANK-AUTOMOTIVE AND ARMAMENTS COMMAND,
     AMSTA-AR-CCB-O, WATERVLIET, NY 12189-4050 OF ADDRESS CHANGES.